

BJP

Bangladesh Journal of Pharmacology

Research Article

Synthesis, molecular modeling, anti-cancer, and COX-1 /2 inhibitory activities of novel thiazolidinones containing benzothiazole core

Synthesis, molecular modeling, anti-cancer and COX-1/2 inhibitory activities of novel thiazolidinones containing benzothiazole core

Necla Kulabas¹, Cansu Tamniku Guven², Merve Duracik³, Ozlem Bingol Ozakpinar³ and Ilkay Kucukguzel⁴

¹Department of Pharmaceutical Chemistry Faculty of Pharmacy, Marmara University, Basibuyuk 34854, Istanbul, Turkey; ²Department of Pharmaceutical Chemistry, Institute of Health Sciences, Marmara University, Kartal 34865, Istanbul, Turkey; ³Department of Biochemistry, Faculty of Pharmacy, Marmara University, Basibuyuk 34854, Istanbul, Turkey; ⁴Department of Pharmaceutical Chemistry, Faculty of Pharmacy, Fenerbahce University, 34758, Istanbul, Turkey.

Article Info

Received: 7 December 2023
Accepted: 2 January 2024
Available Online: 15 March 2024
DOI: 10.3329/bjp.v19i1.70297

Cite this article:

Kulabas N, Guven CT, Duracik M, Bingol Ozakpinar O, Kucukguzel I. Synthesis, molecular modeling, anti-cancer and COX-1/2 inhibitory activities of novel thiazolidinones containing benzothiazole core. Bangladesh J Pharmacol. 2024; 19: 1-12.

Abstract

In this study, new 1,3-thiazolidin-4-one derivatives containing arylmethylene groups in the 5-position were obtained from 6-(trifluoromethoxy)-1,3-benzothiazol-2-amine (riluzole). Synthesized compounds were characterized by spectral data and elemental analysis. *In vitro*, cytotoxic activities of the synthesized molecules were evaluated against the human lung cancer (A549) and human prostate cancer (PC-3) cell lines. Compounds were also tested on mouse embryonic fibroblast cells (NIH/3T3) to determine selectivity. Ten target compounds 3-12 were also screened for their COX-1 and COX-2 inhibitory activities. Of these compounds, 4 showed the highest COX-2 inhibition at 10 μ M. Molecular docking calculations were performed to understand the binding interactions of compounds with COX-1 and COX-2 proteins. *In silico* studies of the tested compounds represented important binding modes that may be responsible for their anti-cancer activity via selective inhibition of the COX-2 enzyme. ADMET predictions were conducted to assess the drug-like properties of the novel compounds.

Introduction

Cancer is one of the most important health problems of the 21st century due to its increasing incidence and high mortality. According to the current data from the World Health Organization, approximately 18.1 million people were diagnosed with cancer in 2018, and 9.6 million people died due to cancer.

Compounds containing 5-arylmethylene-4-thiazolidinone and benzothiazole ring form the core structure of many synthetic compounds with their broad-spectrum biological activity, including anti-cancer effects. 5-arylmethylene-4-thiazolidinone derivatives have been reported in the literature as anti-inflammatory (Eleftheriou et al., 2012; Haroun et al., 2021; Omar et al.,

2020; Ottanà et al., 2007, 2005), antimicrobial (Tatar et al., 2010; Vicini et al., 2006; Vicini et al., 2008) and anti-cancer (Havrylyuk et al., 2010; Ottanà et al., 2005; Zhou et al., 2008) effects (Figure 1). In recent years, promising results have been obtained in terms of anti-cancer effects in the literature. Anti-cancer effects of 5-arylmethylene-4-thiazolidinone derivatives which are responsible for many biological effects including COX-2 enzyme inhibitory effects have been promising for the treatment of cancer and inflammatory diseases (Apostolidis et al., 2013; Türe et al., 2021).

On the other hand, the benzothiazole ring is a heterocycle containing electron-rich sulfur and nitrogen atoms, and compounds bearing benzothiazole rings are



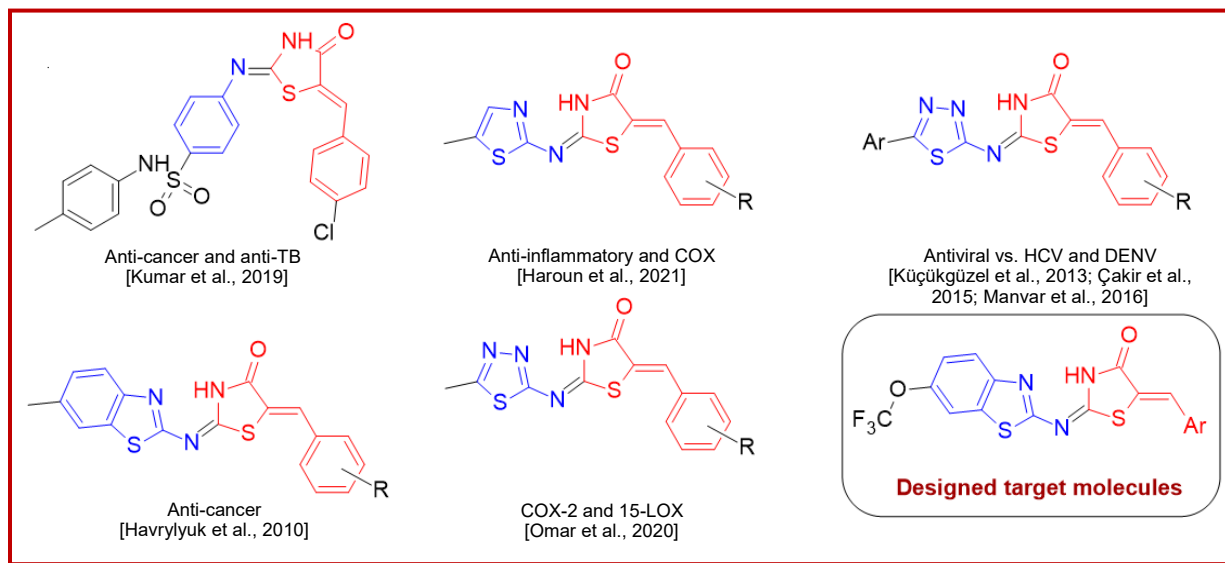


Figure 1: Structures of the reported 1,3-thiazolidine-4-ones and benzothiazole derivatives as biologically active agents and the newly designed benzothiazole-thiazolidinone conjugates

known to have many biological activities. There are numerous reports on the antimicrobial (Catalano et al., 2013; Saeed et al., 2010), anticonvulsant (Liu et al., 2016), anti-inflammatory (Shafi et al., 2012), anti-cancer (Akhtar et al., 2008) activities of benzothiazole derivatives. It has been reported that benzothiazole derivatives are effective on molecular targets such as fatty acid amide hydrolase (FAAH) (Wang et al., 2009), raf kinase (Raf-1) (Song et al., 2008) and BCL-2 (Zheng et al., 2007), especially in the discovery of new anti-cancer agents.

For decades, studies on 2-imino-1,3-thiazolidin-4-one compounds have been ongoing in many research groups. In recent years, a significant increase has been observed in studies conducted with both 2-imino-1,3-thiazolidin-4-one compounds and compounds bearing benzothiazole rings. Many reports reveal that these compounds may be hepatitis C virus NS5B polymerase inhibitors (Çakir et al., 2015; Küçükgül et al., 2013) or dengue virus NS5 (RdRp) inhibitors (Manvar et al., 2016), or anti-cancer agents (Abdellatif et al., 2015; Geronikaki et al., 2008; Havrylyuk et al., 2010; Zhou et al., 2008).

The research described herein is an extension of ongoing efforts toward a search for novel anti-cancer agents bearing the thiazolidinone scaffold. Considering the above-mentioned literature on the biological effects of benzothiazole derivatives, combining the benzothiazole ring and the 5-arylmethylene-1,3-thiazolidin-4-one skeleton in one molecule was considered a promising approach for the development of new drug-like molecules.

In this current study, synthesis of 2-heteroarylimino-5-arylmethylene-1,3-thiazolidin-4-one derivatives starting from 6-(trifluoromethoxy)-1,3-benzothiazol-2-amine,

their anti-cancer effects and COX-1/2 enzyme inhibitory properties are described. The potential interactions of the synthesized compounds with COX-1 and COX-2 target proteins were also investigated by *in silico* molecular modeling techniques.

Materials and Methods

Chemistry

All solvents and reagents were obtained from commercial sources and used without purification. All melting points ($^{\circ}\text{C}$, uncorrected) were determined using Schmelzpunktbestimmer SMP II basic model melting point apparatus. In thin layer chromatography (TLC) studies, 0.2 mm silica gel F-254 (Merck) plates (20 x 20 cm) were used as adsorbent. Two different solvent systems S1 [petroleum ether: ethyl acetate (50:50 v/v)] and S2 [chloroform: acetone (65:35 v/v)] were used in the chromatographic control of the synthesized compounds. The solvent systems used were of a purity that could be used for chromatographic studies. Detection of the compounds was carried out at 254 nm and 366 nm UV lamps. Elemental analyses were obtained using Leco CHNS-932 and were consistent with the assigned structures. Infrared spectra were recorded on a Shimadzu FTIR 8400S and data are expressed in wavenumber ν (cm^{-1}). ^1H NMR and HMBC spectra were recorded on Bruker Avance 300 MHz for the chemical shifts expressed in δ (ppm) downfield from tetramethylsilane (TMS) using $\text{DMSO-}d_6$ as solvent. High-resolution mass spectra were acquired by using Jeol JMS700 instrument.

Synthesis of 2-chloro-N-[6-(trifluoromethoxy)-1,3-benzothiazol-2-yl]acetamide [1]

6-(Trifluoromethoxy)-1,3-benzothiazol-2-amine (10

mmol) was dissolved in dichloromethane. Triethylamine (0.012 mol) was added and stirred under reflux for 30 min. Chloroacetyl chloride (12 mmol) was then slowly added and the medium was refluxed for 7 hours. At the end of the reaction, the flask content was poured into ice, the precipitate was filtered, dried, and purified by crystallization from ethanol (Kulabaş et al., 2022).

Off-white powder. Yield, 44%. TLC %Rf, 68 (S1). M.p. 182°C. FTIR ν_{\max} (cm⁻¹): 3179 (N-H); 3105, 3071 (C-H arom.); 3004, 2952 (C-H aliph.); 1739 (C=O); 1667 (-NH-bend.). ¹H NMR (300 MHz, DMSO-d₆/TMS) δ ppm: 4.49 (2H, s, -COCH₂Cl); 7.43-7.47 (1H, m, ArH); 7.87 (1H, d, *J*=9 Hz, ArH); 8.16 (1H, d, *J*=2.1 Hz, ArH); 12.86 (1H, s, NH). HRMS (EI⁺); (m/z, calcd./found): 309.9785/309.9781 [M]⁺. Anal. calcd. for C₁₀H₆ClF₃N₂O₂S: C, 38.66; H, 1.95; N, 9.02; S, 10.32. Found: C, 38.64; H, 1.964; N, 9.06; S, 9.52.

Synthesis of 2-[[6-(trifluoromethoxy)-1,3-benzothiazol-2-yl]imino]-1,3-thiazolidin-4-one [2]

2-Chloro-N-[6-(trifluoromethoxy)-1,3-benzothiazol-2-yl]acetamide [1] (0.004 mol) was dissolved in ethanol. Ammonium thiocyanate (0.006 mol) was added and boiled under reflux for 7 hours. Afterward, the reaction was terminated by pouring the flask content into ice. The resulting precipitate was filtered, dried, and purified by crystallization from ethanol (Kulabaş et al., 2017).

Gray shiny powder. Yield, 27%. TLC %Rf, 60 (S1); 72 (S2). M.p. 228°C. FTIR ν_{\max} (cm⁻¹): 3140 (N-H); 3063, 2989 (C-H arom.); 2820 (C-H aliph.); 1726, 1699 (C=O). ¹H NMR (300 MHz, DMSO-d₆/TMS) δ ppm: 4.09 (2H, s, -CH₂-thiazolidinone); 7.39-7.46 (1H, m, ArH); 7.88 (1H, d, *J*=9 Hz, ArH); 8.13 (1H, d, *J*=1.2 Hz, ArH); 12.37 (1H, s, NH). HRMS (EI⁺); (m/z, calcd./found): 332.9848/332.9849 [M]⁺. Anal. calcd. for C₁₁H₆F₃N₃O₂S₂.H₂O: C, 37.61; H, 2.30; N, 11.96; S, 18.25. Found: C, 37.52; H, 2.178; N, 13.13; S, 17.81.

Synthesis of 5-(substituted aryl methylene)-2-[[6-(trifluoromethoxy)-1,3-benzothiazol-2-yl]imino]-1,3-thiazolidin-4-ones [3-12]

2-[[6-(Trifluoromethoxy)-1,3-benzothiazol-2-yl]imino]-1,3-thiazolidin-4-one [2] (0.0011 mol) was dissolved in a methanolic solution of equimolar sodium methoxide. An appropriate aromatic/heteroaromatic aldehyde (0.0011 mol) was added to it. The mixture was heated in a water bath under reflux at 90°C for 4 hours. Then, the medium was cooled and neutralized with 10% acetic acid. The crude product was washed thoroughly with water, dried, and then purified by washing with boiling methanol (Çakir et al., 2015; Küçükgülzel et al., 2013).

5-(3-Fluorobenzylidene)-2-[[6-(trifluoromethoxy)-1,3-benzothiazol-2-yl]imino]-1,3-thiazolidin-4-one [3]

Yellow powder. Yield, 33%. TLC %Rf, 80 (S2). M.p. 368-

370°C. FTIR ν_{\max} (cm⁻¹): 3244 (N-H); 3196, 3011 (C-H arom.); 1643 (C=O). ¹H NMR (300 MHz, DMSO-d₆/TMS) δ ppm: 7.19-7.59 (5H, m, ArH); 7.38 (1H, d, *J*=8.7 Hz, ArH); 7.50 (1H, s, =CH-Ar); 7.91 (1H, d, *J*=1.5 Hz, ArH). HRMS (EI⁺); (m/z, calcd./found): 439.0067/439.0050 [M]⁺. Anal. calcd. for C₁₈H₉F₄N₃O₂S₂.3 mol H₂O: C, 43.81; H, 3.06; N, 8.52; S, 13.00. Found: C, 43.69; H, 2.496; N, 8.521; S, 12.17.

5-(4-Chlorobenzylidene)-2-[[6-(trifluoromethoxy)-1,3-benzothiazol-2-yl]imino]-1,3-thiazolidin-4-one [4]

Yellow powder. Yield, 36%. TLC %Rf, 75 (S2). M.p. 287-289°C. FTIR ν_{\max} (cm⁻¹): 3086 (N-H); 3026, 2972 (C-H arom.); 1699, 1688 (C=O). ¹H NMR (300 MHz, DMSO-d₆/TMS) δ ppm: 7.50 (1H, d, *J*=8.7 Hz, ArH); 7.65 (2H, d, *J*=8.7 Hz, ArH); 7.72 (2H, d, *J*=8.7 Hz, ArH); 7.79 (1H, s, =CH-Ar); 8.00 (1H, d, *J*=8.4 Hz, ArH); 8.16 (1H, s, ArH); 13.03 (1H, s, NH). ¹³C NMR (150 MHz, DMSO-d₆/TMS) δ ppm: 115.44 (ArC), 118.35 (C5, thiazolidinone), 120.47 (ArC), 121.83 (=CH-Ar), 122.76, 124.69, 129.43 (ArC), 131.83 (-OCF₃), 134.20, 135.00, 144.62, 149.67, 159.10 (ArC), 166.75 (C2, thiazolidinone), 169.95 (C=O, thiazolidinone). HRMS (DART⁺); (m/z, calcd./found): 455.9777/455.9853 [M+H]⁺. Anal. calcd. for C₁₈H₉ClF₃N₃O₂S₂.3 mol H₂O: C, 46.51; H, 2.17; N, 9.04; S, 13.80. Found: C, 46.42; H, 2.054; N, 8.961; S, 12.60.

5-(4-Methoxybenzylidene)-2-[[6-(trifluoromethoxy)-1,3-benzothiazol-2-yl]imino]-1,3-thiazolidin-4-one [5]

Yellow powder. Yield, 6%. TLC %Rf, 73 (S2). M.p. 238-239°C. FTIR ν_{\max} (cm⁻¹): 3036 (N-H); 3019 (C-H arom.); 2903, 2839 (C-H aliph.); 1713 (C=O). ¹H NMR (300 MHz, DMSO-d₆/TMS) δ ppm: 3.83 (3H, s, -OCH₃); 7.11 (2H, d, *J*=8.7 Hz, ArH); 7.35 (1H, d, *J*=8.4 Hz, ArH); 7.59-7.62 (3H, m, =CH-Ar and ArH); 7.79 (1H, d, *J*=8.4 Hz, ArH); 7.98 (1H, s, ArH). HRMS (EI⁺); (m/z, calcd./found): 451.0267/451.0277 [M]⁺. Anal. calcd. for C₁₉H₁₂F₃N₃O₃S₂. 3/2 mol H₂O: C, 47.80; H, 2.96; N, 8.80; S, 13.43. Found: C, 48.12; H, 2.965; N, 8.852; S, 12.52.

5-(4-Fluorobenzylidene)-2-[[6-(trifluoromethoxy)-1,3-benzothiazol-2-yl]imino]-1,3-thiazolidin-4-one [6]

Yellow powder. Yield, 24%. TLC %Rf, 70 (S2). M.p. 245-247°C. FTIR ν_{\max} (cm⁻¹): 3119 (N-H); 3050, 2997 (C-H arom.); 1717 (C=O). ¹H NMR (300 MHz, DMSO-d₆/TMS) δ ppm: 7.39-7.48 (3H, m, ArH); 7.65-7.77 (3H, m, =CH-Ar and ArH); 7.96 (1H, d, *J*=9 Hz, ArH); 8.12 (1H, s, ArH); 12.98 (1H, s, NH). HRMS (EI⁺); (m/z, calcd./found): 439.0067/439.0059 [M]⁺. Anal. calcd. for C₁₈H₉F₄N₃O₂S₂.1 H₂O: C, 47.26; H, 2.42; N, 9.19; S, 14.02. Found: C, 47.57; H, 2.418; N, 9.087; S, 12.65.

5-(2-Chlorobenzylidene)-2-[[6-(trifluoromethoxy)-1,3-benzothiazol-2-yl]imino]-1,3-thiazolidin-4-one [7]

Yellow powder. Yield, 59%. TLC %Rf, 55 (S2). M.p. 367°C. FTIR ν_{\max} (cm⁻¹): 3090 (N-H); 3040 (C-H arom.); 1647 (C=O). ¹H NMR (300 MHz, DMSO-d₆/TMS) δ ppm: 7.28 (1H, d, *J*=8.7 Hz, ArH); 7.40 (1H, t, *J*=7.5 Hz and

$J=7.8$ Hz, ArH); 7.53 (1H, t, $J=7.2$ Hz and $J=7.8$ Hz, ArH); 7.59 (1H, d, $J=8.1$ Hz, ArH); 7.67-7.73 (2H, m, ArH); 7.74 (1H, s, =CH-Ar); 7.90 (1H, d, $J=1.5$ Hz, ArH). HRMS (DART⁺); (m/z, calcd./found): 455.9844/455.9852 [M+H]⁺. Anal. calcd. for C₁₈H₉ClF₃N₃O₂S₂.1 H₂O: C, 45.62; H, 2.34; N, 8.87; S, 13.53. Found: C, 45.03; H, 1.811; N, 8.688; S, 11.55.

5-(2-Fluorobenzylidene)-2-[[6-(trifluoromethoxy)-1,3-benzothiazol-2-yl]imino]-1,3-thiazolidin-4-one [8]

Yellow powder. Yield, 62%. TLC %Rf, 48 (S2). M.p. 322-323°C. FTIR ν_{\max} (cm⁻¹): 3295 (N-H); 3094, 3050 (C-H arom.); 1647 (C=O). ¹H NMR (300 MHz, DMSO-d₆/TMS) δ ppm: 7.26-7.33 (2H, m, ArH); 7.35-7.47 (2H, m, ArH); 7.59 (1H, s, =CH-Ar); 7.63-7.70 (2H, m, ArH); 7.90 (1H, d, $J=1.5$ Hz, ArH). HRMS (EI⁺); (m/z, calcd./found): 439.0067/439.0071 [M]⁺. Anal. calcd. for C₁₈H₉F₄N₃O₂S₂.3 H₂O: C, 43.81; H, 3.06; N, 8.52; S, 13.00. Found: C, 43.86; H, 2.512; N, 8.485; S, 11.67.

5-(2-Methoxybenzylidene)-2-[[6-(trifluoromethoxy)-1,3-benzothiazol-2-yl]imino]-1,3-thiazolidin-4-one [9]

Yellow powder. Yield, 8%. TLC %Rf, 55 (S2). M.p. 240-242°C. FTIR ν_{\max} (cm⁻¹): 3119 (N-H); 3046 (C-H arom.); 2995, 2791 (C-H aliph.); 1721 (C=O). ¹H NMR (300 MHz, DMSO-d₆/TMS) δ ppm: 3.89 (3H, s, -OCH₃); 7.08-7.12 (2H, m, ArH); 7.28 (1H, d, $J=8.7$ Hz, ArH); 7.38 (1H, t, $J=7.5$ Hz, ArH); 7.55 (1H, d, $J=7.5$ Hz, ArH); 7.68 (1H, d, $J=8.7$ Hz, ArH); 7.80 (1H, s, =CH-Ar); 7.89 (1H, s, Hz ArH). HRMS (DART⁺); (m/z, calcd./found): 452.0345/452.0349 [M+H]⁺. Anal. calcd. for C₁₉H₁₂F₃N₃O₃S₂.1 H₂O: C, 48.61; H, 3.01; N, 8.95; S, 13.66. Found: C, 48.06; H, 2.560; N, 8.769; S, 13.52.

5-(3-Methoxybenzylidene)-2-[[6-(trifluoromethoxy)-1,3-benzothiazol-2-yl]imino]-1,3-thiazolidin-4-one [10]

Yellow powder. Yield, 14%. TLC %Rf, 54 (S2). M.p. 225°C. FTIR ν_{\max} (cm⁻¹): 3092 (N-H); 3196, 3011 (C-H arom.); 2938, 2915 (C-H aliph.); 1701 (C=O). ¹H NMR (300 MHz, DMSO-d₆/TMS) δ ppm: 3.82 (3H, s, -OCH₃); 6.96 (1H, d, $J=7.8$ Hz, ArH); 7.15-7.20 (2H, m, ArH); 7.27 (1H, d, $J=9$ Hz, ArH); 7.41 (1H, t, $J=7.8$ Hz and $J=8.1$ Hz, ArH); 7.46 (1H, s, =CH-Ar); 7.68 (1H, d, $J=8.7$ Hz, ArH); 7.89 (1H, s, Hz ArH). HRMS (EI⁺); (m/z, calcd./found): 451.0267/451.0286 [M]⁺. Anal. calcd. for C₁₉H₁₂F₃N₃O₃S₂: C, 50.55; H, 2.68; N, 9.31; S, 14.21. Found: C, 50.26; H, 2.937; N, 9.223; S, 14.44.

5-(3-Chlorobenzylidene)-2-[[6-(trifluoromethoxy)-1,3-benzothiazol-2-yl]imino]-1,3-thiazolidin-4-one [11]

Yellow powder. Yield, 6%. TLC %Rf, 68 (S2). M.p. 231-233°C. FTIR ν_{\max} (cm⁻¹): 3337 (N-H); 3156, 3101 (C-H arom.); 1705 (C=O). ¹H NMR (300 MHz, DMSO-d₆/TMS) δ ppm: 7.29 (1H, d, $J=8.7$ Hz, ArH); 7.44 (1H, d, $J=8.7$ Hz, ArH); 7.47 (1H, s, ArH); 7.51-7.59 (2H, m, ArH); 7.64 (1H, s, =CH-Ar); 7.69 (1H, d, $J=8.7$ Hz, ArH); 7.90 (1H, s, ArH). HRMS (EI⁺); (m/z, calcd./found): 454.9771/454.9800 [M]⁺. Anal. calcd. for C₁₈H₉ClF₃N₃

O₂S₂: C, 47.43; H, 1.99; N, 9.22; S, 14.07. Found: C, 47.05; H, 2.389; N, 9.083; S, 14.07.

5-[(5-Ethylfuran-2-yl)methylidene]-2-[[6-(trifluoromethoxy)-1,3-benzothiazol-2-yl]imino]-1,3-thiazolidin-4-one [12]

Yellow powder. Yield, 6%. TLC %Rf, 63 (S2). M.p. 255°C. FTIR ν_{\max} (cm⁻¹): 3127 (N-H); 3032, 2978 (C-H arom.); 2901, 2768 (C-H aliph.); 1715 (C=O). ¹H NMR (300 MHz, DMSO-d₆/TMS) δ ppm: 1.36 (3H, t, $J=7.5$ Hz, -CH₂CH₃); 2.84 (2H, q, $J=7.5$ Hz, -CH₂CH₃); 6.46 (1H, d, $J=3.3$ Hz, ArH); 7.08 (1H, d, $J=3.3$ Hz, ArH); 7.50 (1H, d, $J=9.0$ Hz, ArH); 7.55 (1H, s, =CH-Ar); 7.87 (1H, d, $J=8.7$ Hz, ArH); 8.15 (1H, s, ArH); 12.77 (1H, s, NH). HRMS (EI⁺); (m/z, calcd./found): 439.0267/439.0254 [M]⁺. Anal. calcd. for C₁₈H₁₂F₃N₃O₃S₂.1 H₂O: C, 48.21; H, 2.92; N, 9.37; S, 14.30. Found: C, 48.68; H, 2.520; N, 9.347; S, 13.70.

Biological methods

Cell culture

Human lung cancer (A549), human prostate cancer (PC-3), and mouse embryonic fibroblast (NIH/3T3) cell lines were purchased from the American Type Culture Collection (USA). The cells were grown in Dulbecco's modified Eagle medium (DMEM) from Gibco, USA, which contains 10% fetal bovine serum and were kept in an incubator at 37°C and 5% CO₂. At 80-90% confluence, cell passage was carried out (Bülbül et al., 2022).

COX-1/2 inhibitory activity

The inhibitory potential of all synthesized compounds on COX-1 and COX-2 enzymes was evaluated using a COX inhibitor screening kit (Cayman Chemical, USA). The samples and control were dissolved in the DMSO and diluted with the reaction buffer to their final concentrations. DMSO served as a negative control for 100% initial activity. The inhibitor interference by adding the inhibitor to a boiled enzyme sample as a control was tested. The assay was conducted in duplicate and statistical analysis was carried out using GraphPad Prism 6.1 Software (Kulabaş et al., 2023).

Molecular docking studies

The structures of COX-1 (PDB code: 1Q4G, resolution: 2.0 Å) (Gupta et al., 2004) and COX-2 (PDB code: 3LN1, resolution: 2.4 Å) were obtained from the protein data bank (Wang et al., 2010). The target enzymes were prepared for docking studies using the AutoDock Tools program (Morris et al., 2009). Each enzyme was cleaned by removing the water molecules and co-crystallized inhibitors. The charge of the Fe atom in each enzyme was set to +2 manually. To validate the docking protocol, the co-crystallized inhibitors were docked into respective COX enzyme. Binding pockets for the COX-1 enzyme were detected using the CavityPlus web server (Xu et al., 2018; Yuan et al., 2020, 2013). The 3D structures of designed inhibitors were optimized with semi-empirical PM3 method via conformation search in

Box 1: MTT assay**Principle**

The MTT [3-(4,5-dimethylthiazol-2-yl)-2,5-diphenyltetrazolium bromide] assay is a colorimetric method to evaluate the antiproliferative activity. It is based on the conversion of MTT to insoluble formazan crystals by mitochondrial enzymes. This reduction is directly related to the metabolic functionality and viability of the cells tested.

Requirements

3-(4,5-Dimethylthiazol-2-yl)-2,5-diphenyltetrazolium bromide (MTT); Human lung cancer cell line, A549 (ATCC, CCL-185); Human prostate cancer cell line, PC-3 (ATCC, CRL-1435); Microplate reader (BioTek, USA); Mouse embryonic fibroblast cell line, NIH/3T3 (ATCC, CRL-1658); sodium dodecyl sulfate buffer; Incubator; Synthesized compounds; 96-Well plate

Procedure

Step 1: In 96-well plates, the cells (1×10^4 cells/well) were seeded and incubated overnight.

Step 2: After removal of cell media, each culture well was washed with 200 μ L of phosphate buffered saline (PBS) solution and the fresh medium was added. Then, the cells were treated with different concentrations (1-50 μ M) of synthesized compounds 2-12 for 48 hours. At the end of the

incubation, the cell medium was discarded and the wells were cleaned by adding of 200 μ L of PBS. Then, PBS was discarded and 100 μ L of the freshly prepared cell medium was distributed to all wells.

Step 3: MTT was added to each well at a final concentration of 0.5 mg/mL after the initial incubation time and incubated for an additional 4 hours.

Step 4: At the end of 4 hours, the cell media was discarded and 100 μ L sodium dodecyl sulfate (SDS) was added to the wells and incubated at 37°C for 12 hours to dissolve the formazone crystals formed by MTT.

Step 5: Using a microplate reader, absorbances at 570 and 630 nm wavelengths were measured. All tests were repeated three times.

Calculation

The percentage of cell viability was calculated using the equation:

$$[\text{mean OD of treated cells} / \text{mean OD of control cells}] \times 100$$

References

Bülül et al., 2022

References (Video)

Bahuguna et al., 2017

Spartan 4 program and used for initial geometry in docking calculation (Stewart, 2007). The resultant docking files were analyzed to explain the mechanism of binding using BIOVIA Discovery Studio Visualizer program (<https://discover.3ds.com/>).

Calculation of molecular properties

Pharmacokinetic profiles, toxicity risks (mutagenicity, tumorigenicity, irritation, and reproductive effect), and physico-chemical properties (e.g. cLogP, TPSA, drug-score) of compounds were calculated by the methodology developed by OSIRIS Data Warrior software (<http://www.openmolecules.org/datawarrior/>) and ADME properties calculated using SwissADME (<http://www.swissadme.ch/>).

Results**Chemistry****Synthesis and characterization of compounds 1-12**

In the present study, 10 original 5-arylmethylene-2-[[6-(trifluoromethoxy)-1,3-benzothiazol-2-yl]imino]-1,3-thiazolidin-4-one derivatives were synthesized. In the first step, the corresponding chloroacetamide derivative **1** was prepared by reacting 6-(trifluoromethoxy)-1,3-benzothiazol-2-amine with chloroacetyl chloride in the presence of triethylamine. Compound **2**, identified as 2-[[6-(trifluoromethoxy)-1,3-benzothiazol-2-yl]imino]-1,3-thiazolidin-4-one was obtained by refluxing compound **1** with ammonium thiocyanate in an ethanolic medium.

Finally, target compounds **3-12** were synthesized by Knoevenagel condensation of compound **2** with several aromatic aldehydes with the aid of sodium methoxide. All the newly synthesized compounds have been characterized by the use of IR, ^1H NMR, HMBC, and mass spectral data while their purities were proved with TLC and elemental analysis.

In the FTIR spectra of compounds **2-12**, the N-H stretching bands of the thiazolidinone ring had been observed as weak bands in the range of 3036-3337 cm^{-1} , while the C=O stretchings were detected at 1643-1761 cm^{-1} as strong bands. When the ^1H NMR data of the target compounds **2-12** were evaluated, the NH protons of the 4-thiazolidinone ring were detected as broad singlets in the range of 12.37-13.03 ppm. The NH proton of the ring could not be detected in the spectra of compounds **3**, **5**, and **7-11**. It was considered that the NH proton was exchanged by D_2O during the analysis of these compounds and therefore could not be observed. In the ^1H -NMR spectrum of compound **2**, while the singlet appeared at 4.09 ppm corresponding to the active methylene $-\text{CH}_2-$ group, this proton disappeared for the ^1H NMR spectrum of compounds **3-12**.

The ^1H NMR spectra of compounds **3-12** also exhibited a methine proton ($\text{Ar}-\text{CH}=\text{C}<$), which was deshielded by the neighboring C=O moiety and appeared at δ 7.46-7.80 ppm field. Furthermore, the additional four aromatic protons belonging to benzylidene structures were detected between 6.46-7.77 ppm for compounds **3-12**.

In the mass spectra of compounds **1-12** recorded by EI and DART techniques, molecular ion peaks were detected for all compounds. The difference between the calculated and found values was less than 0.05 for each compound, confirming the structures of the compounds.

HMBC analysis was applied to elucidate the carbon skeleton of compound **4**, one of the arylmethylenide derivatives, and thus the structure was determined using ^{13}C - ^1H interactions at two, three, or more bond distances (See Supplementary data). When the 107-128 ppm range of the HMBC spectrum was examined, the chemical shift value of the carbons of the benzothiazole ring (C11, C14, and C15), the carbons of the thiazolidin-4-one ring (C8), and the C1 and C7 carbon of the benzene ring were determined. The C14 carbon of the benzothiazole ring was detected at 115.44 ppm, with two symmetrical contours with the H14 proton attached to it. In the 129-154 ppm range of the spectrum, the chemical shift values of the carbon atoms of the 1,4 disubstituted benzene ring (C2-6) and the carbon atoms of the benzothiazole ring (C10, C12, C13, and C18) were observed and were identified as a result of their coupling with the surrounding hydrogen atoms. The peak observed at 131.83 ppm was attributed to the C18 carbon of the benzothiazole ring due to its contour with the H12 proton around 7.5 ppm, whereas the peak at 144.62 ppm was attributed to the C10 carbon due to its interactions with H14, H11, and H12 hydrogens. The interactions of the C4 carbon with the H2, H3, H5, and H6 protons on the 1,4 disubstituted benzene ring confirmed that this carbon resonated at 135.00 ppm. The C17 carbon atom of the thiazolidin-4-one ring was detected at 166.75 ppm due to its interaction with the methine proton.

Biological studies

Anti-cancer activity

The antiproliferative effects of the synthesized com-

pounds were first investigated on A549 (lung cancer) and PC-3 (prostate cancer) cell lines using the MTT technique. NIH3T3 cells were used to determine the selectivity of the measured cytotoxic effect values. In general, the addition of a benzylidene group to the structure of compound **2** did not create a strong dramatic anti-cancer effect, but it is noteworthy that the most effective derivatives were found with the 4-substitution of benzylidene groups (Table I). Among the screened benzothiazole-thiazolidinone conjugates, compound **5** was determined as the most effective derivative with IC_{50} values of 22.8 μM against A549 cells and 43.4 μM against PC-3 cell lines. The selectivity index of this molecule was determined as 2.5 for A549 cells and 1.5 for PC-3 cells.

Inhibition of COX-1 and COX-2 enzymes

The results obtained in the COX-1/2 inhibition assays of the compounds are given in Table II. Celecoxib was used as a positive control in the present study. According to the enzyme assay results, target molecules **2**, **4**, **5**, and **12** showed more than 70% inhibition against COX-2 at 1 μM . Compound **4** had higher activity compared to celecoxib, while the remaining molecules showed similar or lower activity. Another advantage of the active compounds was that they showed 6% or less inhibition of COX-1 enzyme even at 50 μM concentration and were more selective inhibitors than celecoxib. The binding energies calculated in the molecular docking study reflected the results of *in vitro* inhibition. While high scores were obtained with all arylmethylenide derivatives (**3-12**), it was observed that none of the target molecules could interact with the COX-1 binding pocket. Compound **5**, which had the highest anti-cancer activity, remarkably had a selective inhibition of the COX-2 enzyme. Among the target molecules, the highest COX-2 inhibitory effect was observed in the derivatives carrying chlorine or methoxy at the 4-position, while the substitution shift to other positions slightly decreased the activity. It was understood with compound **12**

Compound	Ar	IC_{50} (μM)		
		A549 cells	PC-3 cells	NIH3T3 cells
2	-	157.53	154.93	129.49
3	3-fluorophenyl	174.22	96.60	227.19
4	4-chlorophenyl	40.70	73.14	28.45
5	4-methoxyphenyl	22.84	43.42	56.73
6	4-fluorophenyl	35.05	38.46	32.47
7	2-chlorophenyl	297.27	112.63	79.13
8	2-fluorophenyl	146.74	94.62	70.03
9	2-methoxyphenyl	113.87	73.56	81.13
10	3-methoxyphenyl	172.30	152.00	73.92
11	3-chlorophenyl	168.95	156.70	92.58
12	5-ethylfuran-2-yl	126.07	120.07	83.25

Table II						
COX-1 and COX-2 enzyme inhibition and the binding energy in the cyclooxygenase active site of synthesized compounds						
Compound	% Inhibition		Docking score ΔG (kcal/mol)			
	COX-1 (50 μ M)	COX-2 (1 μ M)	Pocket A (active site)	Pocket B	Gate Pocket of A	COX-2
2	n.a. ^a	75.8	n.d. ^b	n.d.	-7.8	-8.5
3	n.a.	60.0	n.d.	-9.8	n.d.	-10.8
4	1.7	88.1	n.d.	-9.0	n.d.	-10.4
5	1.0	77.8	n.d.	-9.1	n.d.	-10.7
6	n.a.	63.2	n.d.	-9.2	n.d.	-10.7
7	6.0	65.3	n.d.	-9.7	n.d.	-9.9
8	6.0	65.6	n.d.	-8.1	n.d.	-10.1
9	5.3	64.8	n.d.	-8.9	n.d.	-10.5
10	n.a.	59.5	n.d.	-8.5	n.d.	-10.9
11	5.5	65.8	n.d.	-9.3	n.d.	-10.8
12	6.0	70.0	n.d.	-8.8	n.d.	-9.8
Celecoxib (1 μ M)	27.9	78.7	-10.5	-	-	-12.0

^aNot active, ^bNot detected

that the presence of furylmethylene group instead of benzylidene groups also preserved the inhibitory effect. Compounds **4** and **6**, which were found to have anti-cancer activity, also showed inhibition of COX-2 but were ineffective against COX-1 at 50 μ M. However, it could be said that there was a complete correlation between COX-2 inhibitory properties and anti-cancer activities for all synthesized compounds.

Molecular docking studies

Computer-assisted molecular docking techniques have been utilized to estimate the possible inhibitory activities and mechanism of binding to COX enzymes of the synthesized compounds. The interactions of these compounds with the active site of both COX enzymes were investigated to support enzyme inhibition studies, and celecoxib was used as a reference ligand. Binding energy was obtained from the docking studies of compounds **2-12** by using AutoDock Vina software

(<http://autodock.scripps.edu>). While the binding energies of all synthesized compounds show high affinity to COX-2 active site, not detected bind to the the active site pocket of COX-1 as compatible with the *in vitro* tests in Table II. When the docked conformations of compounds **2-12** in COX-1 in more detail were analyzed, was noticed that bind to different pockets of COX-1 with better affinities, instead of its active site. Using an online tool, CavityPlus web server, four different binding sites A, B, C, and D were identified for COX-1 protein structure (PDB code: 1Q4G) (Figure 2). Compounds **3-12** were found to interact with pocket B at various binding energies while not interacting with the active site identified as pocket A. Similarly, compound **2** also interacted with the gate pocket of A. These findings support the fact that the synthesized compounds have less than 6% inhibition at 50 μ M dose. The docking scores are given in Table II.

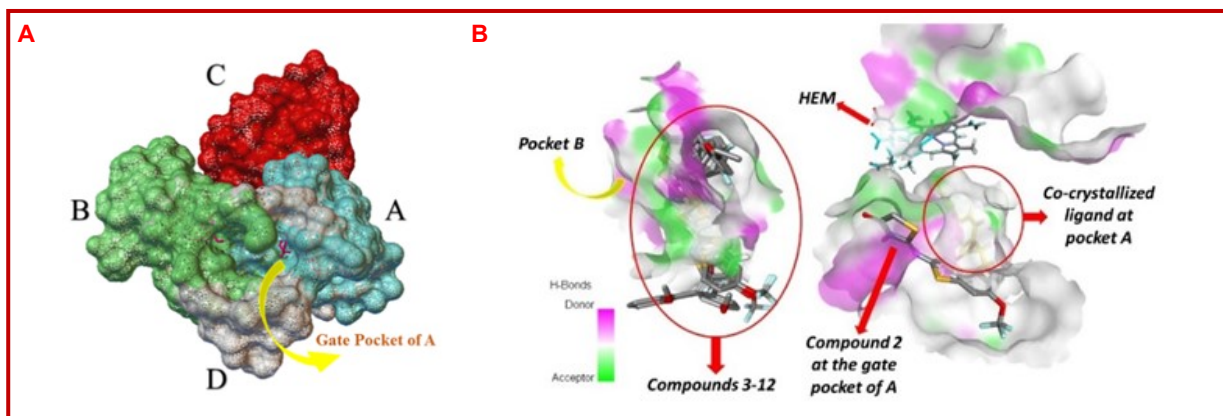


Figure 2: The predicted druggable binding sites of COX-1 according to CavityPlus web server. Pocket A is the cyclooxygenase active site and pocket C is peroxidase binding site (red colored 'A'). Interactions of alternative bindings of compounds **2-12** with the binding sites of COX-1 enzyme (red colored 'B')

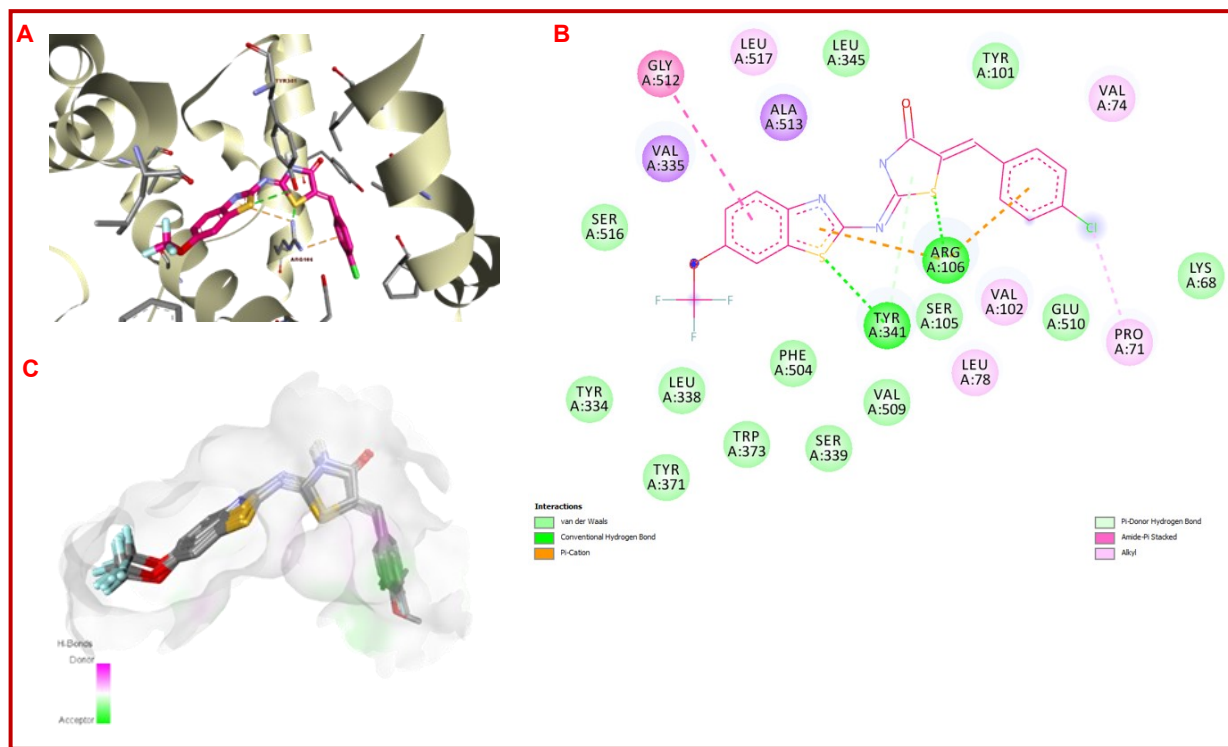


Figure 3: 3D diagram of binding orientation of compound 4 in cyclooxygenase active site of COX-2 (A). 2D diagram of the interaction of the compound 4 with active site of COX-2 enzyme (B). The binding pose of compounds 3-12 at active site of COX-2 enzyme (C)

As the most effective and selective COX-2 inhibitor, the binding orientation and interactions of compound 4 at the COX-2 active site are shown in Figures 3A and 3B. When the interactions of compound 4 were examined, a hydrogen bond between the sulfur atom of the benzothiazole ring and the side chain of Tyr341 was detected. Moreover, two pi-cation interactions were observed between Arg106 and both benzothiazole and arylmethylene aromatic rings. The pi-stacked interaction of Gly512 with benzothiazole ring is thought to promote the inhibitory effect. When the interactions of the synthesized 5-arylmethylene-2-imino-1,3-thiazolidin-4-one derivatives with COX-2 active site were examined, all compounds exhibited similar binding poses with a range of -9.8 via -10.9 kcal/mol binding energy (Figure 3C).

In silico ADMET studies

Oral bioavailability plays an important role in the development of bioactive molecules such as therapeutic agents. For this reason, a computational study was carried out for the prediction of ADME properties by determining the lipophilicity of the molecules, topological polar surface area (TPSA), absorbance (%ABS), simple molecular descriptors using the Lipinski's rule of five (Table III). The calculated number of hydrogen bond donors was 1 for all of the compounds, whilst the number of hydrogen bond acceptors varied from 5 to 6. These new compounds, which can show absorption in

the range of 64.06-81.59%, have a log P value of less than 5, except compounds 4, 7, and 11. Investigation of Lipinski parameters of the synthesized compounds showed that all heterocyclic derivatives of riluzole, compounds 2-12, might be considered drug-like candidates for novel COX-2 inhibitors, as they obeyed the rule of five without violating more than one of them.

Swissadme server was also used for boiled-egg plot denoted (Figure 4). In the graphic yellow area was defined as well penetrated within the brain with good intestinal absorption. The white area was defined as intestinal absorption, while the gray area indicated poor intestinal absorption. None of the synthesized compounds, including compound 2, exhibited the potential to cross the blood-brain barrier, whereas only compound 2 was predicted to be passively absorbed by the gastrointestinal tract. According to the estimated toxicity profiles of the compounds, only compound 12 showed mutagenic effects, while both compound 7 and compound 12 showed tumorigenic profiles. None of the compounds showed irritant properties besides the low reproductive effect detected for compound 8.

Discussion

In this study, 10 new benzothiazole-thiazolidone conjugate compounds were synthesized based on riluzole, a 2-aminobenzothiazole derivative. In the reactions that

Compound	M.W. (g/mol)	cLogP	H-Acceptors	H-Donors	%ABS	TPSA	Drug-likeness
2	333.314	2.72	5	1	68.5936	117.12	-6.4621
3	439.412	4.71	5	1	68.5936	117.12	-5.7999
4	455.867	5.44	5	1	68.5936	117.12	-5.1221
5	451.448	4.76	6	1	65.4093	126.35	-5.1177
6	439.412	4.93	5	1	68.5936	117.12	-5.1839
7	455.867	5.44	5	1	68.5936	117.12	-5.1221
8	439.412	4.93	5	1	68.5936	117.12	-5.1839
9	451.448	4.76	6	1	65.4093	126.35	-5.1177
10	451.448	4.76	6	1	65.4093	126.35	-5.1177
11	455.867	5.44	5	1	68.5936	117.12	-5.1221
12	439.437	4.83	6	1	64.0603	130.26	-3.8862
Riluzole	234.201	2.88	3	1	82.6489	76.38	-8.5405

%ABS: Percentage of absorption - calculated according to the equation %ABS = 109-0.345 x TPSA (Zhao et al., 2002); TPSA: Topological polar surface area

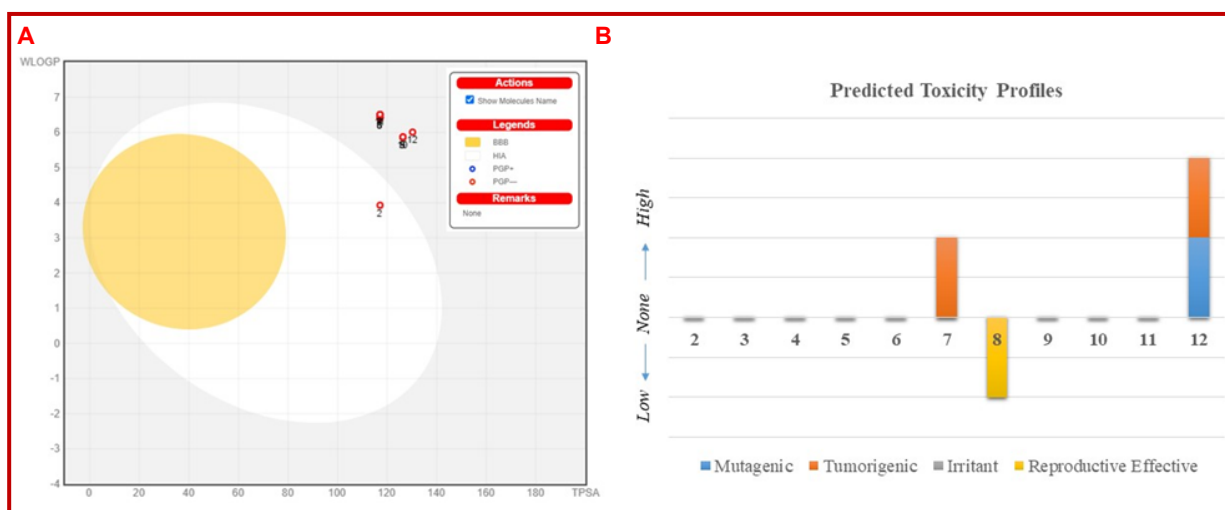
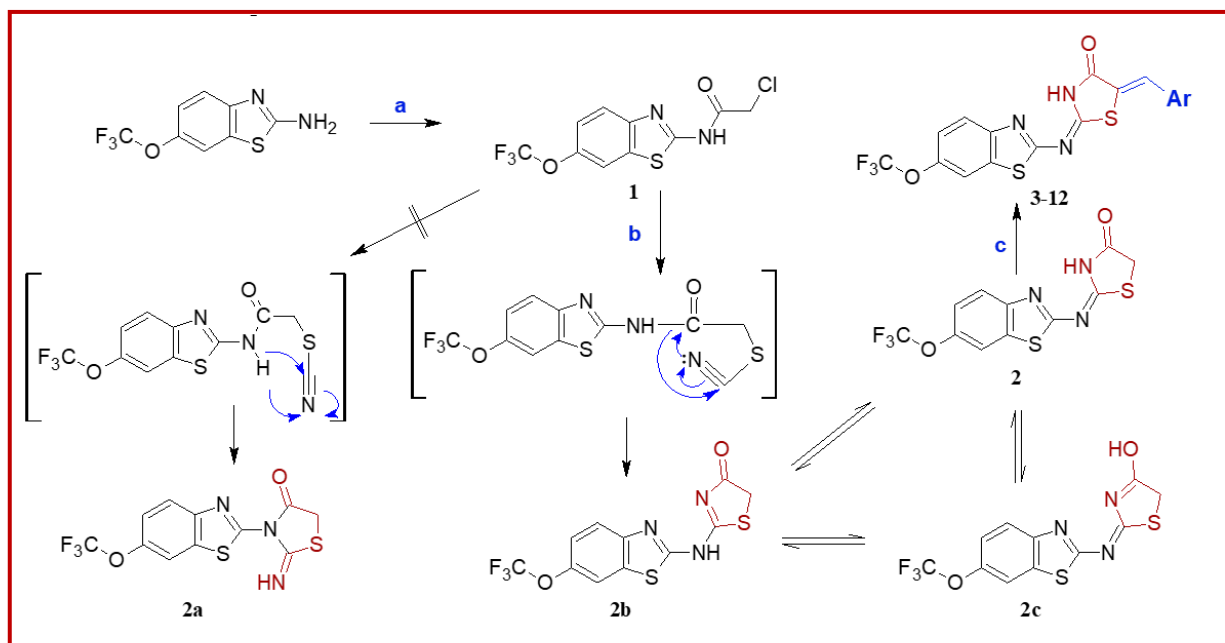


Figure 4: Graphical distribution of compounds according to the boiled-egg predictive model (A), and their toxicity profiles (B)

took place in three steps, first compound **1** was obtained by chloroacetylation, and then compound **2** was obtained by the thiazolidone ring closure. The proposed mechanism of cyclocondensation of compound **1** to compound **2** and its hypothetically tautomeric forms (**2**, **2a-c**) are shown in Scheme 1. The absence of a band that can be attributed to the OH group in the FTIR spectrum, the detection of the NH group of the lactam structure around 3140 cm^{-1} , the detection of the C=O group in the range of 1726-1699 cm^{-1} confirmed that the ring is in the thiazolidinone structure (tautomeric forms **2**, **2a** or **2b**) (Vicini et al., 2008; Havrylyuk et al., 2010). The γ -lactam structure of **2** was confirmed based on the ^1H NMR spectrum which exhibited an NH proton appeared at 12.37 ppm as the previously reported NH resonances appeared around 12-13 ppm. These findings showed that this proton corresponds to a lactam proton of tautomeric form **2** but not to an imine proton of tautomeric form **2a** which is expected to appear at a

much higher field at around 9.0 ppm (Abdellatif et al., 2016; Kulabaş et al., 2017; Türe et al., 2021). In previous studies, it has been reported that these two tautomers cannot be isolated separately experimentally, since the minimum energy change was detected between imino (**2**) \rightleftharpoons amino (**2b**) tautomers, one of the tautomeric forms of the 1,3-thiazolidinone ring (Nowaczyk et al., 2014). The presence of two strong carbonyl bands (1726 cm^{-1} and 1699 cm^{-1}) in the FTIR spectrum of compound **2** can be explained by the presence of two tautomeric forms which 2-amino-4-thiazolinone (**2b**) and the 2-imino-4-thiazolidinone (**2**) structure. Although the presence of both 2-amino-4-thiazolinone (**2b**) and the 2-imino-4-thiazolidinone tautomeric forms (**2**) in solid form is detected in the FTIR spectrum, it is observed that only the 2-imino-4-thiazolidinone form (**2**) is in solution. Additionally, the singlet appeared at 4.09 ppm corresponds to the active methylene $-\text{CH}_2-$ group, supporting the cyclization of the 4-thiazolidinone ring (Küçükgül



Scheme 1: General procedure for the synthesis of compounds **3-12**. Reagents and conditions: a) Cl-CO-CH₂-Cl, TEA, DCM, reflux; b) NH₄SCN, EtOH, reflux; c) Ar-CH=O, NaOMe, MeOH, reflux. **3** (Ar: 3-fluorophenyl); **4** (Ar: 4-chlorophenyl); **5** (Ar: 4-methoxyphenyl); **6** (Ar: 4-fluorophenyl); **7** (Ar: 2-chlorophenyl); **8** (Ar: 2-fluorophenyl); **9** (Ar: 2-methoxyphenyl); **10** (Ar: 3-methoxyphenyl); **11** (Ar: 3-chlorophenyl); **12** (Ar: 5-ethylfuran-2-yl)

et al., 2002; Bekhit et al., 2008).

Target compounds **3-12** were obtained from the Knoevenagel reaction of compound **2** with several aldehydes. Although it has been reported in many studies that this reaction occurs in the presence of sodium acetate/acetic acid (Jung et al., 2011; Rashid et al., 2014), the sodium methoxide/methanol medium was preferred as reported in previous studies (Küçükgülzel et al., 2013; Çakır et al., 2015; Türe et al., 2021). The findings indicating that the target compounds **3-12** were obtained are the detection of an additional four aromatic protons belonging to benzylidene structures and methine proton (=CH-Ar) between 6.46-7.77 ppm and 7.46-7.80 ppm, respectively. Moreover, -CH₂- protons which belong to the thiazolidinone ring of compound **2**, at 4.09 ppm were not observed in the spectrum of compounds **3-12**. When the *E* and *Z* geo-metric isomers of the C=C exocyclic double bond in the 5th position of benzylidene derivatives were examined, the =CH-Ar proton of compounds **3-12** was detected between 7.46-7.80 ppm. In many previously reported studies, the =CH-Ar proton detected in the range of 6.90-7.97 ppm was reported as the *Z* isomer, while the related proton for *E* isomer was reported to be detected in the higher energy area (about 6 ppm) (Havrylyuk et al., 2010; Mushtaque et al., 2012; Ottanà et al., 2005; Vicini et al., 2008, 2006). This finding confirms that the target compounds **3-12** prefer the (*Z*)-isomer due to the -C=C-bond.

Anti-cancer and anti-inflammatory effects of hybrid

compounds containing thiazole, thiadiazole, and benzothiazole rings and 4-thiazolidinone rings in the same structure have been reported in the literature (Havrylyuk et al., 2010). Therefore, the cytotoxic effects and COX-1/2 enzyme inhibition potential of the synthesized compounds were examined on A549 and PC-3 cells. Among compounds **2-12** whose anti-cancer effects were examined by the MTT technique, only compounds **4-6** showed higher activity on A549 and PC-3 cells compared to the others. However, when the effects of these compounds on cancer cells were compared to their effects on NIH3T3 cells, which are healthy, it was observed that their selectivity indexes were low. Therefore, further mechanistic studies on these compounds were not deemed necessary.

Looking at the structure-activity relationships, it was understood that the benzylidene group at the 5-position of the 1,3-thiazolidin-4-one ring represented by compound **2** was necessary for activity, but no effect was observed with 2- or 3-substitution in the benzylidene group. The highest cytotoxic effect was achieved in the presence of halogen or methoxy at the 4-position of the benzylidene group. There is widespread knowledge that the COX-2 enzyme has a crucial role in various solid tumors. Therefore, this enzyme is targeted by medicinal chemists in anti-cancer drug development studies (Şenkardeş et al., 2020).

In the inhibition studies conducted on COX-1 and COX-2 enzymes, it was noteworthy that compounds **4-6**, which had the highest antiproliferative activity, also

selectively inhibited the COX-2 enzyme at high rates. Compound **5** had a higher effect than celecoxib used as a reference, with an inhibition value of 88.1% at 1 μ M concentration. Although there was no exact correlation between the COX-1 and COX-2 enzyme inhibitions of the studied compounds and their docking scores, it was observed that the compounds showing high binding scores mostly selectively inhibited the COX-2 enzyme. A modeling study focusing on compound **4**, which is the most effective and selective COX-2 inhibitor, showed that binding of both benzothiazole and thiazolidone rings with sulfur atoms as hydrogen bond acceptors was effective in binding the inhibitors to the COX-2 active site. In addition, benzothiazole and benzylidene rings were bound to the COX-2 enzyme by pi-cation interaction.

Lipinski's rule of five states that most drug-like molecules with good membrane permeability should have $\log P \leq 5$, formula weight ≤ 500 , number of hydrogen bond acceptors (nON) ≤ 10 and number of hydrogen bond donors (nOHNH) ≤ 5 . Violation of more than one rule indicates problems with bioavailability. Polar surface area, together with lipophilicity, is an important property of a molecule in transport across biological membranes. Too high TPSA values give rise to poor bioavailability and absorption of a drug (Lipinski et al., 1997; Veber et al., 2002). An increase in hydrogen bond acceptors resulted in a slight decrease in the calculated %ABS for compounds **5**, **9**, **10**, and **12**.

There were no direct correlations observed between simple molecular properties such as $\log P$ and anti-cancer or COX-1/2 inhibitory activity. Nevertheless, it was notable that compound **4**, the most active COX-2 inhibitor, had the highest $\log P$ value among the series.

Conclusion

Ten novel benzothiazole-thiazolidinone hybrids **3-12**, were synthesized and characterized in detail by the use of IR, ^1H NMR, HMBC, and MS spectral techniques. Compounds **4-6** containing 4-substitution at arylmethylene moiety exhibited the highest cytotoxic activity towards A549 and PC-3 cell lines, whereas all synthesized compounds inhibited COX-2 enzyme selectively at 1 μ M. Molecular docking studies reveal the binding interactions and justify selective inhibition of COX-2 enzyme by compounds **3-12**.

Financial Support

Self-funded

Ethical Issue

Cell lines derived from expansion of primary cell cultures *in*

vitro are not relevant material, as all of the original cells will have divided and so the cell line has been created outside of the human body. The storage and use of cell lines created from primary human tissue, for research purposes, does not require an ethical approval.

Conflict of Interest

Authors declare no conflict of interest

Acknowledgement

The authors are grateful to Dr. Jurgen Gross from the Institute of Organic Chemistry, University of Heidelberg, for his generous help on obtaining high resolution mass spectra of the compounds.

References

- Abdellatif KRA, Abdelall EKA, Abdelgawad MA, Abdelhakeem MM, Omar HA. Design and synthesis of certain novel arylidene thiazolidinone derivatives as anti-cancer agents. *Der Pharma Chem.* 2015; 7: 149-61.
- Abdellatif KRA, Abdelgawad MA, Elshemy HAH, Alsayed SSR. Design, synthesis and biological screening of new 4-thiazolidinone derivatives with promising COX-2 selectivity, anti-inflammatory activity and gastric safety profile. *Bioorg Chem.* 2016; 64: 1-12.
- Akhtar T, Hameed S, Al-Masoudi NA, Loddo R, La Colla P. *In vitro* antitumor and antiviral activities of new benzothiazole and 1,3,4-oxadiazole-2-thione derivatives. *Acta Pharm.* 2008; 58: 135-49.
- Apostolidis I, Liaras K, Geronikaki A, Hadjipavlou-Litina D, Gavalas A, Soković M, Glamočlija J, Ćirić A. Synthesis and biological evaluation of some 5-arylidene-2-(1,3-thiazol-2-ylimino)-1,3-thiazolidin-4-ones as dual anti-inflammatory/antimicrobial agents. *Bioorg Med Chem.* 2013; 21: 532-39.
- Bahuguna A, Khan I, Bajpai VK, Kang SC. MTT assay to evaluate the cytotoxic potential of a drug. *Bangladesh J Pharmacol.* 2017; 12: 115-18.
- Bülbü l B, Ding K, Zhan CG, Çiftçi G, Yelekc i K, Gürboğa M, Özakpınar ÖB, Aydemir E, Baybağ D, Şahin F, Kulabaş N, Helvacioğlu S, Charehsaz M, Tatar E, Özbey S, Küçükgüzel İ. Novel 1,2,4-triazoles derived from ibuprofen: Synthesis and *in vitro* evaluation of their mPGES-1 inhibitory and antiproliferative activity. *Mol Divers.* 2022: (early access).
- Çakır G, Küçükgüzel I, Guhamazumder R, Tatar E, Manvar D, Basu A, Patel BA, Zia J, Talele TT, Kaushik-Basu N. Novel 4-thiazolidinones as non-nucleoside inhibitors of hepatitis C virus NS5B RNA-dependent RNA polymerase. *Arch Pharm (Weinheim).* 2015; 348: 10-22.
- Catalano A, Carocci A, Defrenza I, Muraglia M, Carrieri A, Van Bambeke F, Rosato A, Corbo F, Franchini C. 2-Aminobenzothiazole derivatives: Search for new antifungal agents. *Eur J Med Chem.* 2013; 64: 357-64.
- Eleftheriou P, Geronikaki A, Hadjipavlou-Litina D, Vicini P, Filz O, Filimonov D, Poroikov V, Chaudhaery SS, Roy KK, Saxena AK. Fragment-based design, docking, synthesis, bio-

- logical evaluation and structure-activity relationships of 2-benzo/benzisothiazolimino-5-arylidene-4-thiazolidinones as cyclooxygenase/lipoxygenase inhibitors. *Eur J Med Chem.* 2012; 47: 111-24.
- Geronikaki A, Eleftheriou P, Vicini P, Alam I, Dixit A, Saxena AK. 2-Thiazolylimino/Heteroarylino-5-arylidene-4-thiazolidinones as new agents with SHP-2 inhibitory action. *J Med Chem.* 2008; 51: 1.
- Gupta K, Selinsky BS, Kaub CJ, Katz AK, Loll PJ. The 2.0 Å resolution crystal structure of prostaglandin H2 synthase-1: Structural insights into an unusual peroxidase. *J Mol Biol.* 2004; 335: 503-18.
- Haroun M, Tratat C, Petrou A, Geronikaki A, Ivanov M, Ciric A, Sokovic M. 2-Aryl-3-(6-trifluoromethoxy)benzo[d]thiazole-based thiazolidinone hybrids as potential anti-infective agents: Synthesis, biological evaluation and molecular docking studies. *Bioorg Med Chem Lett.* 2021; 32: 127718.
- Havrylyuk D, Mosula L, Zimenkovsky B, Vasylenko O, Gzella A, Lesyk R. Synthesis and anti-cancer activity evaluation of 4-thiazolidinones containing benzothiazole moiety. *Eur J Med Chem.* 2010; 45: 5012-21.
- Jung ME, Ku JM, Du L, Hu H, Gatti RA. Synthesis and evaluation of compounds that induce readthrough of premature termination codons. *Bioorg Med Chem Lett* 2011; 21: 5842-48.
- Küçükgülzel I, Satılmış G, Gurukumar KR, Basu A, Tatar E, Nichols DB, Talele TT, Kaushik-Basu N. 2-Heteroarylino-5-arylidene-4-thiazolidinones as a new class of non-nucleoside inhibitors of HCV NS5B polymerase. *Eur J Med Chem.* 2013; 69: 931-41.
- Kulabaş N, Özakpınar ÖB, Özsvacı D, Leyssen P, Neyts J, Küçükgülzel İ. Synthesis, characterization and biological evaluation of thioureas, acylthioureas and 4-thiazolidinones as anti-cancer and antiviral agents. *Marmara Pharm J.* 2017; 21: 371-84.
- Kulabaş N, Set İ, Aktay G, Gürsoy Ş, Daniş Ö, Ogan A, Sağ Erdem S, Erzincan P, Helvacıoğlu S, Hamitoğlu M, Küçükgülzel İ. Identification of some novel amide conjugates as potent and gastric sparing anti-inflammatory agents: *In vitro*, *in vivo*, *in silico* studies and drug safety evaluation. *J Mol Struct.* 2023; 1285.
- Kulabaş N, Türe A, Bozdeveci A, Krishna VS, Alpay Karaoğlu Ş, Sriram D, Küçükgülzel İ. Novel fluoroquinolones containing 2-arylamino-2-oxoethyl fragment: Design, synthesis, evaluation of antibacterial and antituberculosis activities and molecular modeling studies. *J Heterocycl Chem.* 2022; 59: 909-26.
- Kumar AS, Kudva J, Bharath BR, Ananda K, Sadashiva R, Madan Kumar S, Revanasiddappa BC, Kumar V, Rekha PD, Naral D. Synthesis, structural, biological and *in silico* studies of new 5-arylidene-4-thiazolidinone derivatives as possible anti-cancer, antimicrobial and antitubercular agents. *New J Chem.* 2019; 43: 1597-610.
- Lipinski CA, Lombardo F, Dominy BW, Feeney PJ. Experimental and computational approaches to estimate solubility and permeability in drug discovery and development settings. *Adv Drug Deliv Rev.* 1997; 23: 3-25.
- Liu DC, Zhang HJ, Jin CM, Quan ZS. Synthesis and biological evaluation of novel benzothiazole derivatives as potential anticonvulsant agents. *Molecules* 2016; 21: 164.
- Manvar D, Küçükgülzel I, Erensoy G, Tatar E, Deryabaşoullari G, Reddy H, Talele TT, Cevik O, Kaushik-Basu N. Discovery of conjugated thiazolidinone-thiadiazole scaffold as anti-dengue virus polymerase inhibitors. *Biochem Biophys Res Commun.* 2016; 469: 743-47.
- Morris GM, Huey R, Lindstrom W, Sanner MF, Belew RK, Goodsell DS, Olson AJ. Software news and updates gabedit: A graphical user interface for computational chemistry softwares. *J Comput Chem.* 2009; 30: 174-82.
- Mushtaque M, Avecilla F, Azam A. Synthesis, characterization and structure optimization of a series of thiazolidinone derivatives as *Entamoeba histolytica* inhibitors. *Eur J Med Chem.* 2012; 55: 439-48.
- Nowaczyk A, Kowiel M, Gzella A, Fijałkowski Ł, Horishny V, Lesyk R. Conformational space and vibrational spectra of 2-[(2,4-dimethoxyphenyl) amino]-1,3-thiazolidin-4-one. *J Mol Model.* 2014; 20: 2366.
- Omar YM, Abdel-Moty SG, Abdu-Allah HHM. Further insight into the dual COX-2 and 15-LOX anti-inflammatory activity of 1,3,4-thiadiazole-thiazolidinone hybrids: The contribution of the substituents at 5th positions is size dependent. *Bioorg Chem.* 2020; 97: 103657.
- Ottanà R, Maccari R, Barreca ML, Bruno G, Rotondo A, Rossi A, Chiricosta G, Di Paola R, Sautebin L, Cuzzocrea S, Vigorita MG. 5-Arylidene-2-imino-4-thiazolidinones: Design and synthesis of novel anti-inflammatory agents. *Bioorg Med Chem.* 2005; 13: 4243-52.
- Ottanà R, Maccari R, Ciurleo R, Vigorita MG, Panico AM, Cardile V, Garufi F, Ronsisvalle S. Synthesis and *in vitro* evaluation of 5-arylidene-3-hydroxyalkyl-2-phenylimino-4-thiazolidinones with antidegenerative activity on human chondrocyte cultures. *Bioorg Med Chem.* 2007; 15: 7618-25.
- Rashid M, Husain A, Shaharyar M, Mishra R, Hussain A, Afzal O. Design and synthesis of pyrimidine molecules endowed with thiazolidin-4-one as new anticancer agents. *Eur J Med Chem.* 2014; 83: 630-45.
- Saeed S, Rashid N, Jones PG, Ali M, Hussain R. Synthesis, characterization and biological evaluation of some thiourea derivatives bearing benzothiazole moiety as potential antimicrobial and anti-cancer agents. *Eur J Med Chem.* 2010; 45: 1323-31.
- Şenkardeş S, Han Mİ, Kulabaş N, Abbak M, Çevik Ö, Küçükgülzel İ, Küçükgülzel ŞG. Synthesis, molecular docking and evaluation of novel sulfonyl hydrazones as anti-cancer agents and COX-2 inhibitors. *Mol Divers.* 2020; 24: 673-89.
- Shafi S, Mahboob Alam M, Mulakayala N, Mulakayala C, Vanaja G, Kalle AM, Pallu R, Alam MS. Synthesis of novel 2-mercapto benzothiazole and 1,2,3-triazole based bis-heterocycles: Their anti-inflammatory and anti-nociceptive activities. *Eur J Med Chem.* 2012; 49: 324-33.
- Song EY, Kaur N, Park MY, Jin Y, Lee K, Kim G, Lee KY, Yang JS, Shin JH, Nam KY, No KT, Han G. Synthesis of amide and urea derivatives of benzothiazole as Raf-1 inhibitor. *Eur J Med Chem.* 2008; 43: 1519-24.
- Stewart JJP. Optimization of parameters for semiempirical

- methods V: Modification of NDDO approximations and application to 70 elements. *J Mol Model*. 2007; 13: 1173-213.
- Tatar E, Küçükgülzel İ, Küçükgülzel ŞG, Feyza Y, Clercq E De, Andrei G, Snoeck R, Pannecouque C, Fikretin Ş, Bayrak ÖF. Synthesis, anti-tuberculosis and antiviral activity of novel 2-isonicotinoylhydrazono-5-arylidene-4-thiazolidinones. *Int J Drug Des Discov*. 2010; 1: 19-32.
- Türe A, Ergül Mustafa, Ergül Merve, Altun A, Küçükgülzel İ. Design, synthesis, and anti-cancer activity of novel 4-thiazolidinone-phenylaminopyrimidine hybrids. *Mol Divers*. 2021; 25: 1025-50.
- Veber DF, Johnson SR, Cheng HY, Smith BR, Ward KW, Kopple KD. Molecular properties that influence the oral bioavailability of drug candidates. *J Med Chem*. 2002; 45: 2615-23.
- Vicini P, Geronikaki A, Anastasia K, Incerti M FZ. Synthesis and antimicrobial activity of novel 2-thiazolylimino-5-arylidene-4-thiazolidinones. *Bioorg Med Chem*. 2006; 14: 3859-64.
- Vicini P, Geronikaki A, Incerti M, Zani F, Dearden J, Hewitt M. 2-Heteroarylimino-5-benzylidene-4-thiazolidinones analogues of 2-thiazolylimino-5-benzylidene-4-thiazolidinones with antimicrobial activity: Synthesis and structure-activity relationship. *Bioorg Med Chem*. 2008; 16: 3714-24.
- Wang JL, Limburg D, Graneto MJ, Springer J, Hamper JRB, Liao S, Pawlitz JL, Kurumbail RG, Maziasz T, Talley JJ, Kiefer JR, Carter J. The novel benzopyran class of selective cyclooxygenase-2 inhibitors. Part 2: The second clinical candidate having a shorter and favorable human half-life. *Bioorg Med Chem Lett*. 2010; 20: 7159-63.
- Wang X, Sarris K, Kage K, Zhang D, Brown SP, Kolasa T, Surowy C, El Kouhen OF, Muchmore SW, Brioni JD, Stewart AO. Synthesis and evaluation of benzothiazole-based analogues as novel, potent, and selective fatty acid amide hydrolase inhibitors. *J Med Chem*. 2009; 52: 170-80.
- Xu Y, Wang S, Hu Q, Gao S, Ma X, Zhang W, Shen Y, Chen F, Lai L, Pei J. CavityPlus: A web server for protein cavity detection with pharmacophore modelling, allosteric site identification and covalent ligand binding ability prediction. *Nucleic Acids Res*. 2018; 46: W374-79.
- Yuan Y, Pei J, Lai L. LigBuilder V3: A multi-target de novo drug design approach. *Front Chem*. 2020; 8: 1083-91.
- Yuan Y, Pei J, Lai L. Binding site detection and druggability prediction of protein targets for structure-based drug design. *Curr Pharm Des*. 2013; 19: 2326-33.
- Zhao YH, Abraham MH, Le J, Hersey A, Luscombe CN, Beck G, Sherborne B, Cooper I. Rate-limited steps of human oral absorption and QSAR studies. *Pharm Res*. 2002; 19: 1446-57.
- Zheng CH, Zhou YJ, Zhu J, Ji HT, Chen J, Li YW, Sheng CQ, Lu JG, Jiang JH, Tang H, Song YL. Construction of a three-dimensional pharmacophore for Bcl-2 inhibitors by flexible docking and the multiple copy simultaneous search method. *Bioorganic Med Chem*. 2007; 15: 6407-17.
- Zhou H, Wu S, Zhai S, Liu A, Sun Y, Li R, Zhang Y, Ekins S, Swaan PW, Fang B, Zhang B, Yan B. Design, synthesis, cytoselective toxicity, structure-activity relationships, and pharmacophore of thiazolidinone derivatives targeting drug-resistant lung cancer cells. *J Med Chem*. 2008; 51: 1242-51.

Author Info

Ilkay Kucukguzel (Principal contact)
e-mail: kucukguzel@hotmail.com